C.P. No. 385
(18,755)
A.R.C. Technical Report

C.P. No. 385
(18,755)
A.R.C. Technical Report

MINISTRY OF SUPPLY

AERONAUTICAL RESEARCH COUNCIL

CURRENT PAPERS

Calculation of the shape of a Thin Slender Wing for a Given Load Distribution and Planform

By

J. H. B. Smith, M.Sc.

LONDON: HER MAJESTY'S STATIONERY OFFICE

1958

PRICE 3s. 6d. NET

C.P. No. 385

U.D.C. No. 533.691.13 : 533.69.048.1

Technical Note No. Aero 2410

January, 1956

ROYAL AIRCRAFT ESTABLISHMENT

Calculation of the shape of a thin slender wing for a given load distribution and planform

by

J. H. B. Smith, M.Sc.

SUMMARY

The problem considered in this note is that of finding the camber and twist for a swept wing of specified slender planform which will produce the same chordwise lift distribution at each spanwise station as in two-dimensional flow past a flat plate, in conjunction with a uniform distribution of chord loading. Linearised inviscid potential flow theory is used and the results are valid only if $A^2 |1 - M^2| << 1$. The slope of the wing is obtained in closed form as a function of two rectangular co-ordinates for wings with straight swept leading and trailing edges and streamwise tips. Numerical results are given for the chordwise and spanwise variations of the slope of the wing surface measured in the chordwise (that is, the streamwise) direction, at several stations, and chordwise wing sections are drawn, for two particular planforms. These sections are found to have continuous tangents and not more than three discontinuities of curvature. Spanwise distributions of camber and local incidence are given for the two wings.

LIST OF CONTENTS

		Page
1	Introduction	3
2	Evaluation of the surface slope integral	3
3	Numerical results for two planforms	13
4	Discussion	14
List of Symbols		15
References		16

LIST OF ILLUSTRATIONS

	Figure
Planforms for numerical calculation	1
Ranges of integration	2
Types of sub-division of the half-wing	3
Chordwise variation of α/C_L	4
Sweepwise variation of α/C_L	5
Chordwise wing sections	6
Spanwise local incidence distribution	7
Spanwise camber distribution	8

1 Introduction

In connection with the design of a model for wind tunnel tests, the problem was posed of determining the shape of a wing of given planform necessary to produce a uniform distribution of chord loading*, across the span, together with a chordwise lift distribution equal to that occurring in the two-dimensional flow round a flat plate. A uniform distribution of chord loading was assumed in order to produce results for the slope (or downwash) in a closed form. This leads to unrealistic values of the surface slope close to the wing tip, but was thought to be a worthwhile first step in spite of this. The wing planforms considered are restricted to straight swept leading and trailing edges with straight streamwise tips but are otherwise general. The calculation is made under the assumptions of inviscid potential flow at small incidence and the condition $A^2 \left| 1 - M^2 \right| << 1$, which may be interpreted as a restriction to small aspect ratio at any Mach number or to sonic velocity at any aspect ratio.

Under these conditions the problem has already been reduced[1,2] to the evaluation of an integral for the downwash. This leads to elementary, though complicated, functions; the numerical calculation of these presents no difficulty in principle but is involved in practice. Accordingly numerical results were obtained for two planforms only, one tapered and one untapered, of the same aspect ratio and leading edge sweep (Fig.1). The values of β/C_L were found for the wing sections at five spanwise stations with some intermediate points on the leading and trailing edges. From these, five chordwise sections were drawn. Curves were also obtained for the spanwise variation of the local incidence and camber**.

2 Evaluation of the surface slope integral

The function to be evaluated is

$$\beta = -\frac{w}{V} = -\frac{1}{4\pi} \iint_{S^*} \ell(x',y') \frac{dx'\, dy'}{(y-y')^2} \qquad (1)$$

where $\beta = \beta(x,y)$ is the required surface slope, w the perturbation velocity measured upwards normal to the wing in a flow of undisturbed velocity V, S* is that part of the wing lying forward of the point (x,y) and $\ell(x',y')$ is the non-dimensional load distribution. This relation may be found in reference 2.

---

* Chord loading $= \int_{x_\ell(y)}^{x_t(y)} \ell(x,y)\, dx$, a function of y only.

** The local incidence is defined as the angle of inclination of the chord at any spanwise station to the undisturbed flow. The chord at any station is defined as the line joining the leading and trailing edges. The camber is defined as the maximum ordinate of the wing above its chord at the given station expressed as a percentage of the length of the chord.

The load distribution assumed is

$$\ell(x,y) = \frac{\ell_o c_o}{c}\sqrt{\frac{1-\xi}{\xi}} \qquad (2)$$

where c is the local chord, c_o the centre-line chord, ℓ_o a dimensionless constant and ξ a dimensionless co-ordinate varying from 0 along the leading edge to 1 along the trailing edge, defined in (3). This gives the same chordwise lift distribution at each spanwise station as in two-dimensional flow past a flat plate and a uniform distribution of chord loading. A dimensionless spanwise co-ordinate η is also introduced:

$$\left.\begin{aligned} c\,\xi &= x - x_\ell = x - y/K_\ell\,, \quad s\eta = y \\ c'\xi' &= x' - x_\ell' = x' - y'/K_\ell, \quad s\eta' = y' \end{aligned}\right\} \qquad (3)$$

The lines along which ξ is constant will be said to be in the sweepwise direction, as the lines of constant x and y or η are called spanwise and chordwise respectively. Substituting from (2) and (3) in (1) produces

$$\beta = -\frac{\ell_o c_o}{4\pi s}\iint_{S^*}\sqrt{\frac{1-\xi'}{\xi'}}\,\frac{d\xi'\,d\eta'}{(\eta-\eta')^2} \qquad (4)$$

The lift coefficient is given by

$$C_L = \iint_S \ell\,\frac{dx\,dy}{S} = \frac{c_o \ell_o s}{S}\int_{-1}^{1}\left\{\int_0^1\sqrt{\frac{1-\xi'}{\xi'}}\,d\xi'\right\}d\eta'$$

$$= \frac{c_o \ell_o s\pi}{2S}\int_{-1}^{1} d\eta' = \frac{c_o \ell_o s\pi}{S} = \frac{\pi \ell_o}{1+\lambda}$$

so that

$$\ell_o = \frac{1+\lambda}{\pi} C_L \qquad (5)$$

where S is the wing area and λ the taper ratio.

The part S* of the wing area S which lies forward of the pivotal point (x,y) is divided, for purposes of integration, into strips in the direction of constant ξ (i.e. sweepwise) as shown in Fig.2. If the pivotal point (x,y) is upstream of the tip leading edge (i.e. $K_\ell x < s$), all such strips end on the line $x' = x$, at the point where

$$y' = \eta' s = \pm K(x - c_o \xi') = \pm \frac{K_t K_\ell (x - c_o \xi')}{K_\ell \xi' + K_t(1 - \xi')} .$$

Otherwise, if the pivotal point is downstream of the tip leading edge (i.e. $K_\ell x > s$), those strips for which $\lambda K_\ell c_o \xi' < K_\ell x - s$ end at the wing tip where $\eta' = \pm 1$, and the remainder on the line $x' = x$. Hence equation (4) becomes:

$$-\frac{4 \pi s \beta}{\ell_o c_o} = \int_0^{\xi_1} \sqrt{\frac{1 - \xi'}{\xi'}} \left\{ \int_{-1}^{0} \frac{d\eta'}{(\eta - \eta')^2} + \int_0^{1} \frac{d\eta'}{(\eta - \eta')^2} \right\} d\xi'$$

$$+ \int_{\xi_1}^{\xi_2} \sqrt{\frac{1 - \xi'}{\xi'}} \left\{ \int_{-\bar{\eta}}^{0} \frac{d\eta'}{(\eta - \eta')^2} + \int_0^{\bar{\eta}} \frac{d\eta'}{(\eta - \eta')^2} \right\} d\xi' \qquad (6)$$

where $\bar{\eta}\, s(K_\ell \xi' + K_t(1 - \xi')) = K_t K_\ell (x - c_o \xi')$

and $$\lambda K_\ell c_o \xi_1 = \begin{cases} 0 & \text{for } K_\ell x \leq s \\ K_\ell x - s & \text{for } K_\ell x > s \end{cases}$$

as explained above. The second limit of integration, ξ_2, is given by

$$c_o \xi_2 = \begin{cases} x & \text{for } x \leq c_o \\ c_o & \text{for } x > c_o \end{cases}$$

since the second integral must be taken over all strips lying forward of the pivotal point i.e. over all $x' = c_o \xi' \leq x$ if the pivotal point is upstream of the entire wake or $x' = c_o \xi' \leq c_o$ otherwise.

Performing the integration with respect to η' and taking the Cauchy principal value at $\eta' = \eta$ produces:

$$-\frac{4\pi s\,\beta}{\ell_o\,\sigma_o} = -\frac{2}{1-\eta^2}\int_o^{\xi_1}\sqrt{\frac{1-\xi'}{\xi'}}\,d\xi'$$

$$-\int_{\xi_1}^{\xi_2}\sqrt{\frac{1-\xi'}{\xi'}}\,\frac{K_\ell\,\xi' + K_t(1-\xi')}{K_\ell y\,\xi' + K_t y(1-\xi') + K_t\,K_\ell(x - c_o\,\xi')}\,s\,d\xi'$$

$$+\int_{\xi_1}^{\xi_2}\sqrt{\frac{1-\xi'}{\xi'}}\,\frac{K_\ell\,\xi' + K_t(1-\xi')}{K_\ell y\,\xi' + K_t y(1-\xi') - K_t\,K_\ell(x - c_o\,\xi')}\,s\,d\xi'$$

$$= -\frac{2}{1-\eta^2}\int_o^{\xi_1}\sqrt{\frac{1-\xi'}{\xi'}}\,d\xi' - \frac{2(1-\lambda)}{1-\eta^2(1-\lambda)^2}\int_{\xi_1}^{\xi_2}\sqrt{\frac{1-\xi'}{\xi'}}\,d\xi'$$

$$+\frac{s - K_\ell x(1-\lambda)}{K_\ell\,c_o(1-\eta(1-\lambda))^2}\int_{\xi_1}^{\xi_2}\frac{1}{\xi' - a_1}\sqrt{\frac{1-\xi'}{\xi'}}\,d\xi'$$

$$+\frac{s - K_\ell x(1-\lambda)}{K_\ell\,c_o(1+\eta(1-\lambda))^2}\int_{\xi_1}^{\xi_2}\frac{1}{\xi' - a_2}\sqrt{\frac{1-\xi'}{\xi'}}\,d\xi' \qquad (7)$$

Since $K_t\,K_\ell\,c_o(1-\lambda) = (K_t - K_\ell)s$

where $a_1 = \dfrac{K_\ell x - y}{K_\ell\,c_o(1-\eta(1-\lambda))}$ and $a_2 = \dfrac{K_\ell x + y}{K_\ell\,c_o(1+\eta(1-\lambda))}$

The standard integrals involved are:

$$\int\sqrt{\frac{1-\xi'}{\xi'}}\,d\xi' = \sqrt{\xi'(1-\xi')} + \tan^{-1}\sqrt{\frac{\xi'}{1-\xi'}} + \text{const.}$$

$$\frac{1}{2}\int\frac{1}{\xi'-a}\sqrt{\frac{1-\xi'}{\xi'}}\,d\xi' = -\begin{cases}\sqrt{\dfrac{1-a}{a}}\,\log\left|\dfrac{\sqrt{a(1-\xi')} + \sqrt{(1-a)\xi'}}{\sqrt{\xi'-a}}\right| - \tan^{-1}\sqrt{\dfrac{\xi'}{1-\xi'}} & (a<1)\\[2ex] \sqrt{\dfrac{a-1}{a}}\,\tan^{-1}\sqrt{\dfrac{(a-1)\xi'}{a(1-\xi')}} - \tan^{-1}\sqrt{\dfrac{\xi'}{1-\xi'}} & (a>1)\end{cases}$$

Now $a_1 < 1$ for all points of the wing, but $a_2 > 1$ for points of the right (left)-hand half-wing downstream of the extended trailing edge of the left (right)-hand half-wing.

The lines $a_2 = 1$, $K_\ell x = s$ and $x = c_o$ divide the wing into a number of regions in each of which β is given by a different expression. $\beta(x,y)$ is continuous over the entire wing with the exception of the centre-line and wing tips. At the vertex it has a singularity like $Z^{-\frac{1}{2}}$ elsewhere on the centre-line like log Z and at the tips like Z^{-1}. It is differentiable over the entire wing except for $y = 0, \pm s$ and possibly $a_2 = 1$, $K_\ell x = s$, $x = c_o$. Hence the chordwise wing sections have continuous tangents and up to three points of discontinuity in curvature.

The division of the wing into regions takes a different form for a wing of a different shape. Half-wings representative of the two cases possible with swept back leading and trailing edges are shown in figure 3. (Region B may not occur in some cases of the first type). The values taken by the parameters in the various regions are

Region	A	B	C	D	E	F
ξ_1	0	0	>0	>0	>0	0
ξ_2	<1	<1	<1	<1	1	1
a_2	<1	>1	<1	>1	>1	>1

The values of β for the right-hand half-wing for the various regions are obtained from equation (7) in the form below, using equation (5) and $4s = (1 + \lambda) A c_o$.

/Region A:

Region A:

$$\frac{\Lambda \pi^2 \beta}{2C_L} = \frac{1-\lambda}{1-\eta^2(1-\lambda)^2} \sqrt{\frac{x}{c_o}\left(1-\frac{x}{c_o}\right)}$$

$$+ \tan^{-1}\sqrt{\frac{x}{c_o - x}} \left\{ \frac{1-\lambda}{1-\eta^2(1-\lambda)^2} + \frac{s - K_\ell\, x(1-\lambda)}{K_\ell\, c_o(1+\eta(1-\lambda))^2} + \frac{s - K_\ell x(1-\lambda)}{K_\ell\, c_o(1-\eta(1-\lambda))^2} \right\}$$

$$+ \frac{s - K_\ell x(1-\lambda)}{K_\ell\, c_o(1+\eta(1-\lambda))^2} \sqrt{\frac{K_\ell\, c_o(1+\eta(1-\lambda))}{K_\ell x + y} - 1} \log \left| \frac{\sqrt{(K_\ell x + y)(c_o - x)} + \sqrt{x(K_\ell\, c_o(1+\eta(1-\lambda)) - K_\ell x - y)}}{\sqrt{c_o\, \eta(K_\ell x(1-\lambda) - s)}} \right|$$

$$+ \frac{s - K_\ell x(1-\lambda)}{K_\ell\, c_o(1-\eta(1-\lambda))^2} \sqrt{\frac{K_\ell\, c_o(1-\eta(1-\lambda))}{K_\ell x - y} - 1} \log \left| \frac{\sqrt{(K_\ell x - y)(c_o - x)} + \sqrt{x(K_\ell\, c_o(1-\eta(1-\lambda)) - K_\ell x + y)}}{\sqrt{c_o\, \eta(K_\ell x(1-\lambda) - s)}} \right|$$

Region B:

$$\frac{A\,\pi^2\,\beta}{2C_L} = \frac{1-\lambda}{1-\eta^2(1-\lambda)^2}\sqrt{\frac{x}{c_o}\left(1-\frac{x}{c_o}\right)}$$

$$+\tan^{-1}\sqrt{\frac{x}{c_o-x}}\left\{\frac{1-\lambda}{1-\eta^2(1-\lambda)^2}+\frac{s-K_\ell x(1-\lambda)}{K_\ell\, c_o(1+\eta(1-\lambda))^2}+\frac{s-K_\ell x(1-\lambda)}{K_\ell\, c_o(1-\eta(1-\lambda))^2}\right\}$$

$$+\frac{s-K_\ell x(1-\lambda)}{K_\ell\, c_o(1-\eta(1-\lambda))^2}\sqrt{\frac{K_\ell\, c_o(1-\eta(1-\lambda))}{K_\ell x-y}-1}\,\log\left|\frac{\sqrt{(K_\ell x-y)(c_o-x)}+\sqrt{x(K_\ell\, c_o(1-\eta(1-\lambda))-K_\ell x+y}}{\sqrt{c_o\eta(K_\ell x(1-\lambda)-s)}}\right|$$

$$-\frac{s-K_\ell x(1-\lambda)}{K_\ell\, c_o(1+\eta(1-\lambda))^2}\sqrt{1-\frac{K_\ell\, c_o(1+\eta(1-\lambda))}{K_\ell x+y}}\,\tan^{-1}\sqrt{\frac{x}{c_o-x}\left(1-\frac{K_\ell\, c_o(1+\eta(1-\lambda))}{K_\ell x+y}\right)}$$

Region C:

$$\frac{A\pi^2\beta}{2C_L} = \left\{ \frac{1}{1-\eta^2} - \frac{1-\lambda}{1-\eta^2(1-\lambda)^2} \right\} \frac{\sqrt{(K_\ell x - s)(\lambda K_\ell c_o - K_\ell x + s)}}{\lambda K_\ell c_o} + \frac{1-\lambda}{1-\eta^2(1-\lambda)^2} \sqrt{\frac{x}{c_o}\left(1-\frac{x}{c_o}\right)}$$

$$+ \left\{ \frac{1-\lambda}{1-\eta^2(1-\lambda)^2} + \frac{s - K_\ell x(1-\lambda)}{K_\ell c_o(1-\eta(1-\lambda))^2} + \frac{s - K_\ell x(1-\lambda)}{K_\ell c_o(1+\eta(1-\lambda))^2} \right\} \tan^{-1} \sqrt{\frac{x}{c_o - x}}$$

$$+ \left\{ \frac{1}{1-\eta^2} - \frac{1-\lambda}{1-\eta^2(1-\lambda)^2} - \frac{s - K_\ell x(1-\lambda)}{K_\ell c_o(1-\eta(1-\lambda))^2} - \frac{s - K_\ell x(1-\lambda)}{K_\ell c_o(1+\eta(1-\lambda))^2} \right\} \tan^{-1} \sqrt{\frac{K_\ell x - s}{\lambda K_\ell c_o - K_\ell x + s}}$$

$$+ \frac{s - K_\ell x(1-\lambda)}{K_\ell c_o(1-\eta(1-\lambda))^2} \sqrt{\frac{K_\ell c_o(1-\eta(1-\lambda))}{K_\ell x - y} - 1} \log \left| \sqrt{\frac{K_\ell(1-\eta)}{\eta}} \times \frac{\sqrt{(K_\ell x - y)(c_o - x)} + \sqrt{x(K_\ell c_o(1-\eta(1-\lambda)) - K_\ell x + y)}}{\sqrt{(K_\ell x - y)(\lambda K_\ell c_o - K_\ell x + s)} + \sqrt{(K_\ell x - s)(K_\ell c_o(1-\eta(1-\lambda)) - K_\ell x + y)}} \right|$$

$$+ \frac{s - K_\ell x(1-\lambda)}{K_\ell c_o(1+\eta(1-\lambda))^2} \sqrt{\frac{K_\ell c_o(1+\eta(1-\lambda))}{K_\ell x + y} - 1} \log \left| \sqrt{\frac{K_\ell(1+\eta)}{\eta}} \times \frac{\sqrt{(K_\ell x + y)(c_o - x)} + \sqrt{x(K_\ell c_o(1+\eta(1-\lambda)) - K_\ell x - y)}}{\sqrt{(K_\ell x + y)(\lambda K_\ell c_o - K_\ell x + s)} + \sqrt{(K_\ell x - s)(K_\ell c_o(1+\eta(1-\lambda)) - K_\ell x - y)}} \right|$$

Region D:

$$\frac{A\,\pi^2\,\beta}{2C_L} = \left\{ \frac{1}{1-\eta^2} - \frac{1-\lambda}{1-\eta^2(1-\lambda)^2} \right\} \frac{\sqrt{(K_\ell x - s)(\lambda\, K_\ell\, c_o - K_\ell x + s)}}{\lambda\, K_\ell\, c_o} + \frac{1-\lambda}{1-\eta^2(1-\lambda)^2} \sqrt{\frac{x}{c_o}\left(1 - \frac{x}{c_o}\right)}$$

$$+ \left\{ \frac{1-\lambda}{1-\eta^2(1-\lambda)^2} + \frac{s - K_\ell x(1-\lambda)}{K_\ell\, c_o (1-\eta(1-\lambda))^2} + \frac{s - K_\ell x(1-\lambda)}{K_\ell\, c_o (1+\eta(1-\lambda))^2} \right\} \tan^{-1} \sqrt{\frac{x}{c_o - x}}$$

$$+ \left\{ \frac{1}{1-\eta^2} - \frac{1-\lambda}{1-\eta^2(1-\lambda)^2} - \frac{s - K_\ell x(1-\lambda)}{K_\ell\, c_o (1-\eta(1-\lambda))^2} - \frac{s - K_\ell x(1-\lambda)}{K_\ell\, c_o (1+\eta(1-\lambda))^2} \right\} \tan^{-1} \sqrt{\frac{K_\ell x - s}{\lambda\, K_\ell\, c_o - K_\ell x + s}}$$

$$+ \frac{s - K_\ell x(1-\lambda)}{K_\ell\, c_o (1-\eta(1-\lambda))^2} \sqrt{\frac{K_\ell\, c_o (1-\eta(1-\lambda))}{K_\ell x - y} - 1} \quad \log \left| \sqrt{\frac{K_\ell(1-\eta)}{\eta}} \frac{\sqrt{(K_\ell x - y)(c_o - x)} + \sqrt{x(K_\ell\, c_o (1-\eta(1-\lambda) - K_\ell x + y)}}{\sqrt{(K_\ell x - y)(\lambda\, K_\ell\, c_o - K_\ell x + s)} + \sqrt{(K_\ell x - s)(K_\ell\, c_o (1-\eta(1-\lambda)) - K_\ell x + y)}} \right|$$

$$- \frac{s - K_\ell x(1-\lambda)}{K_\ell\, c_o (1+\eta(1-\lambda))^2} \sqrt{1 - \frac{K_\ell\, c_o (1+\eta(1-\lambda))}{K_\ell x + y}} \left\{ \tan^{-1} \sqrt{\frac{(K_\ell x + y - K_\ell\, c_o (1+\eta(1-\lambda)))x}{(K_\ell x + y)(c_o - x)}} - \tan^{-1} \sqrt{\frac{(K_\ell x + y - K_\ell\, c_o (1+\eta(1-\lambda)))(K_\ell x - s)}{(K_\ell x + y)(\lambda\, K_\ell\, c_o - K_\ell x + s)}} \right\}$$

Region E:

$$\frac{A\pi^2\beta}{2C_L} = \left\{ \frac{1}{1-\eta^2} - \frac{1-\lambda}{1-\eta^2(1-\lambda)^2} \right\} \frac{\sqrt{(K_\ell x - s)(\lambda K_\ell c_o - K_\ell x + s)}}{\lambda K_\ell c_o}$$

$$+ \left\{ \frac{1}{1-\eta^2} - \frac{1-\lambda}{1-\eta^2(1-\lambda)^2} - \frac{s - K_\ell x(1-\lambda)}{K_\ell c_o(1+\eta(1-\lambda))^2} - \frac{s - K_\ell x(1-\lambda)}{K_\ell c_o(1-\eta(1-\lambda))^2} \right\} \tan^{-1} \sqrt{\frac{K_\ell x - s}{\lambda K_\ell c_o - K_\ell x + s}}$$

$$+ \frac{\pi}{2} \left\{ \frac{1-\lambda}{1-\eta^2(1-\lambda)^2} + \frac{s - K_\ell x(1-\lambda)}{K_\ell c_o} \left(\frac{1}{(1+\eta(1-\lambda))^2} + \frac{1}{(1-\eta(1-\lambda))^2} - \frac{1}{(1+\eta(1-\lambda))^2} \sqrt{1 - \frac{K_\ell c_o(1+\eta(1-\lambda))}{K_\ell x + y}} \right) \right\}$$

$$+ \frac{s - K_\ell x(1-\lambda)}{K_\ell c_o(1+\eta(1-\lambda))^2} \sqrt{1 - \frac{K_\ell c_o(1+\eta(1-\lambda))}{K_\ell x + y}} \tan^{-1} \sqrt{\frac{(K_\ell x - s)(K_\ell x + y - K_\ell c_o(1+\eta(1-\lambda)))}{(K_\ell x + y)(\lambda K_\ell c_o - K_\ell x + s)}}$$

$$- \frac{s - K_\ell x(1-\lambda)}{K_\ell c_o(1-\eta(1-\lambda))^2} \sqrt{\frac{K_\ell c_o(1-\eta(1-\lambda))}{K_\ell x - y} - 1} \log \left| \frac{\sqrt{(K_\ell x - y)(\lambda K_\ell c_o - K_\ell x + s)} + \sqrt{(K_\ell x - s)(K_\ell c_o(1-\eta(1-\lambda)) - K_\ell x + y)}}{\sqrt{K_\ell c_o(1-\eta)(s - K_\ell x(1-\lambda))}} \right|$$

Region F:

$$\frac{A\pi^2\beta}{2C_L} = \frac{\pi}{2} \left\{ \frac{1-\lambda}{1-\eta^2(1-\lambda)^2} + \frac{s - K_\ell x(1-\lambda)}{K_\ell c_o} \left(\frac{1}{(1+\eta(1-\lambda))^2} + \frac{1}{(1-\eta(1-\lambda))^2} - \frac{1}{(1+\eta(1-\lambda))^2} \sqrt{1 - \frac{K_\ell c_o(1+\eta(1-\lambda))}{K_\ell x + y}} \right) \right\}$$

It is of interest to compare the result for region F when $\lambda = 1$ and A tends to infinity with that for an infinite sheared wing. In region F, for $\lambda = 1$,

$$\frac{A\pi^2\beta}{2C_L} = \frac{\pi}{2}\cdot\frac{s}{K_\ell c_o}\left(2 - \sqrt{1 - \frac{K_\ell c_o}{K_\ell x + y}}\right)\cdot\frac{1}{A}$$

$$= \frac{\pi}{2}\cdot\frac{1}{2K_\ell}\left(2 - \sqrt{1 - \frac{2K_\ell}{2K_\ell\xi + A\eta}}\right) \to \frac{\pi}{4K_\ell} \quad \text{as } A \to \infty$$

Thus in this case $C_L = 2\pi K_\ell \beta$. For an infinite sheared wing $C_L = 2\pi \cos\Lambda\,\alpha$, so that the results agree in the limit of a slender wing, for which $\Lambda \to \pi/2$, since in this case the surface slope is the incidence ($\beta = \alpha$).

3 Numerical results for two planforms

The planforms considered are determined by the following parameters and illustrated in Fig.1.

(a) Tapered wing $K_\ell = 0.7175$ $A = 2.677$ $\lambda = 0.3100$

(b) Untapered wing $K_\ell = 0.7175$ $A = 2.677$ $\lambda = 1.000$

Both wings are of the type shown in Fig.3(b) so that regions A, B, E and F occur. The values of β/C_L for the points of five spanwise stations at $\eta = 0.2$, 0.4, 0.571, 0.74 and 0.9 and at some additional leading and trailing edge points were calculated for each. These are shown in Figs.4 and 5. The values of β/C_L for flat plates of the same planforms as obtained by Mangler[1] are shown for comparison.

Fig.6 gives graphs of the ordinates at these stations under the assumption of no dihedral on the quarter-chord line. The function

$$\frac{z}{cC_L} = -\int_{0.25}^{\xi}\frac{\beta(\xi')d\xi'}{C_L} \qquad (\beta \text{ in radians}),$$

evaluated numerically, is plotted against ξ. With the scales chosen the graphs also portray the wing profiles for $C_L = 2$.

The local incidence is plotted against the spanwise co-ordinate in Fig.7. This provides a picture of the twist of the wing. The camber is plotted in Fig.8 against the spanwise coordinate. For spanwise stations outboard of the point at which the line $K_\ell x = s$ meets the trailing edge (see Fig.3(b)), the chordwise section tends to become S-shaped owing to the rapid increase in the surface slope downstream of this line. This configuration is analogous to that of a wing with flap and so, for these sections, the fore part of the wing, ahead of $K_\ell x = s$, has been treated separately from the aft part for the calculation of camber and twist. The local incidence in the two parts has been taken as the incidence of the lines joining the point of inflexion to the leading and trailing edges. The camber has been taken as the maximum height of the fore (aft) part of the wing above the line joining the point of inflexion to the leading (trailing) edge as a

percentage of the length of this line. Thus in figures 7 and 8 separate curves are shown for the fore and aft parts of the wing for $\eta > 0.417$ on the tapered wing and $\eta > 0.464$ on the untapered wing. The analogy to the wing and flap is not exact since there is no kink in the wing surface corresponding to the hinge of a flap, but only the line of points of inflexion of the wing sections.

4 Discussion

A slender wing with straight swept leading and trailing edges having a two-dimensional chordwise load distribution and a uniform distribution of chord loading has the following features:

(a) The surface slope has no finite discontinuity although its derivatives have. Thus all the wing sections are smooth but may have discontinuities in curvature.

(b) The surface slope tends to infinity as the centre-line is approached, since here the lines of constant loading, and so the bound vortices, are kinked.

(c) The slope rises sharply downstream of the tip leading edge as would be expected since the flat plate solution produces no load in this region.

(d) Starting from the leading edge, the slope decreases along the forward part of a chordwise section.

(e) Along the leading edge, towards the tip, the behaviour of the slope depends on the taper, increasing rapidly for a highly tapered wing but decreasing for the constant chord wing chosen. This result and that in (d) may be made plausible by comparing the load distribution chosen with that for a flat delta wing. The latter is (R.T. Jones[3])

$$\ell_d \propto \sqrt{\frac{x}{x^2 - x_\ell^2}}$$

so that, using equation (2):

$$\frac{\ell_d}{\ell} \propto \sqrt{\frac{xc}{(x + x_\ell)(x_t - x)}}$$

This expression increases with x along a chordwise section and increases or decreases along the leading edge as xc increases or decreases.

(f) The modifications in the chordwise sections produced by substituting the two-dimensional for the flat plate loading are small in the region upstream of the tip leading edge and considerable downstream of it.

List of Symbols

A	aspect ratio
a_1, a_2	parameters occurring in equation (7)
c	local chord
c_o	centre-line chord
C_L	lift coefficient
K_ℓ	cotangent of the leading edge sweep
K_t	cotangent of the trailing edge sweep
K	cotangent of the local sweep $\left(K = \dfrac{K_t K_\ell}{K_\ell \xi + K_t(1-\xi)}\right)$
$\ell = \ell(x,y)$	non-dimensional load distribution
s	semi-span
S	wing area
V	undisturbed velocity
w	perturbation velocity normal to wing measured upwards
x,y	co-ordinates in plane of wing, x measured streamwise and y to starboard
β	slope of wing in streamwise direction
λ	taper ratio $\left(\lambda = 1 - \dfrac{K_t - K_\ell}{K_t K_\ell} \cdot \dfrac{s}{c_o}\right)$
$\xi = \frac{1}{c}(x - y/K_\ell)$	non-dimensional sweepwise co-ordinate
$\eta = y/s$	non-dimensional spanwise co-ordinate

REFERENCES

No.	Author	Titles, etc.
1	K.W. Mangler	Calculation of the pressure distribution over a wing at sonic speeds R. & M. 2868 September, 1951
2	K.W. Mangler	Calculation of the load distribution over a wing with arbitrary camber and twist at sonic speed RAE Report Aero 2515 (1954) ARC 17262
3	R.T. Jones	Properties of low aspect ratio pointed wings at speeds below and above the speed of sound NACA Report No. 835 (1946) ARC 9483 NACA/TN/ 1032; NACA/TIB/966

WT.2078.C.P.385.K3 - Printed in Great Britain.

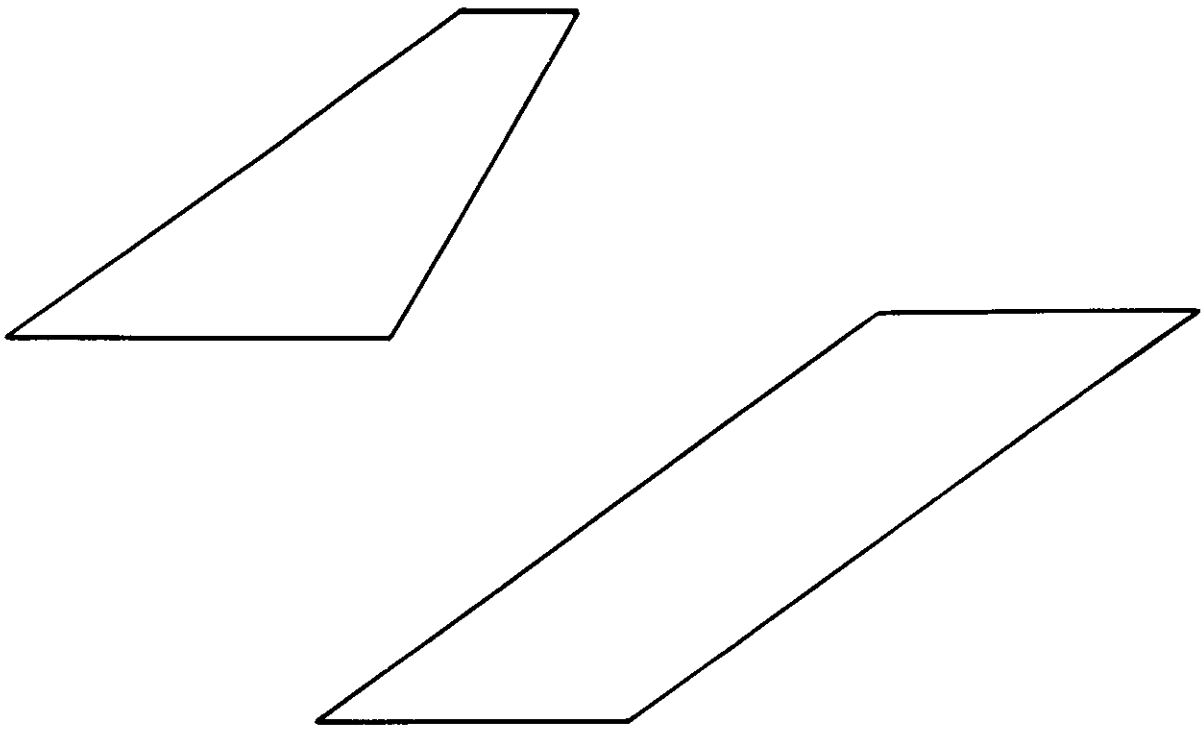

FIG.1. PLANFORMS FOR NUMERICAL CALCULATION.

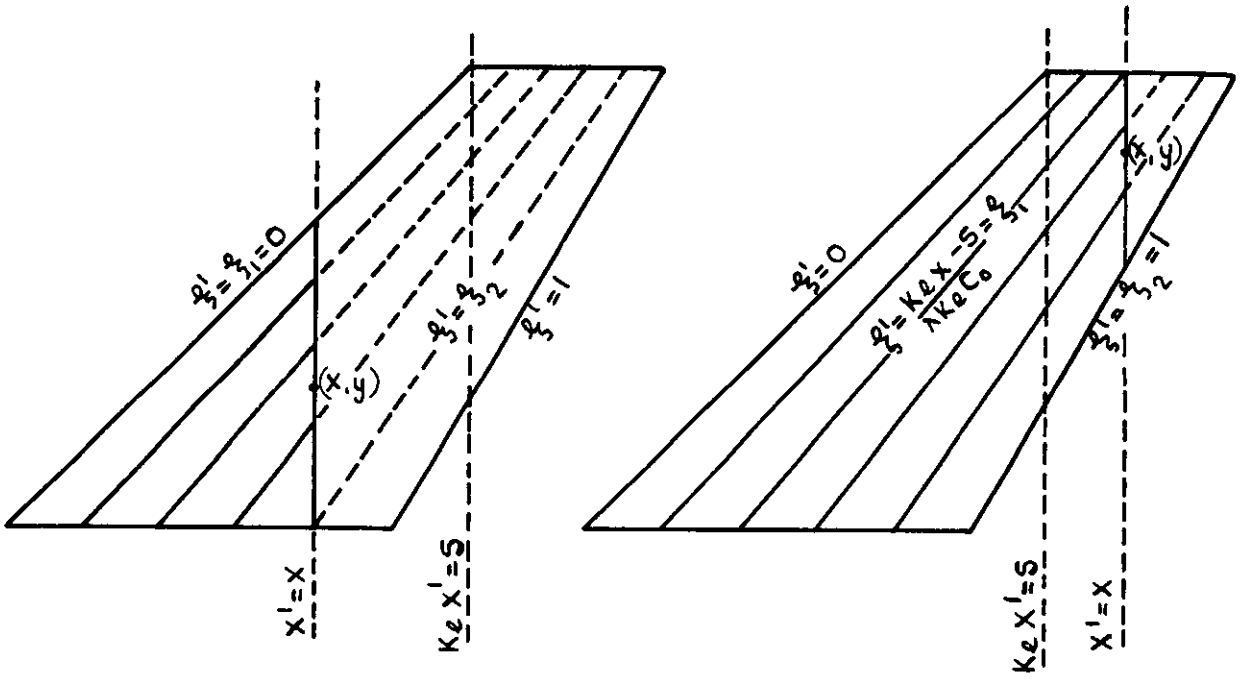

FIG. 2. RANGES OF INTEGRATION.

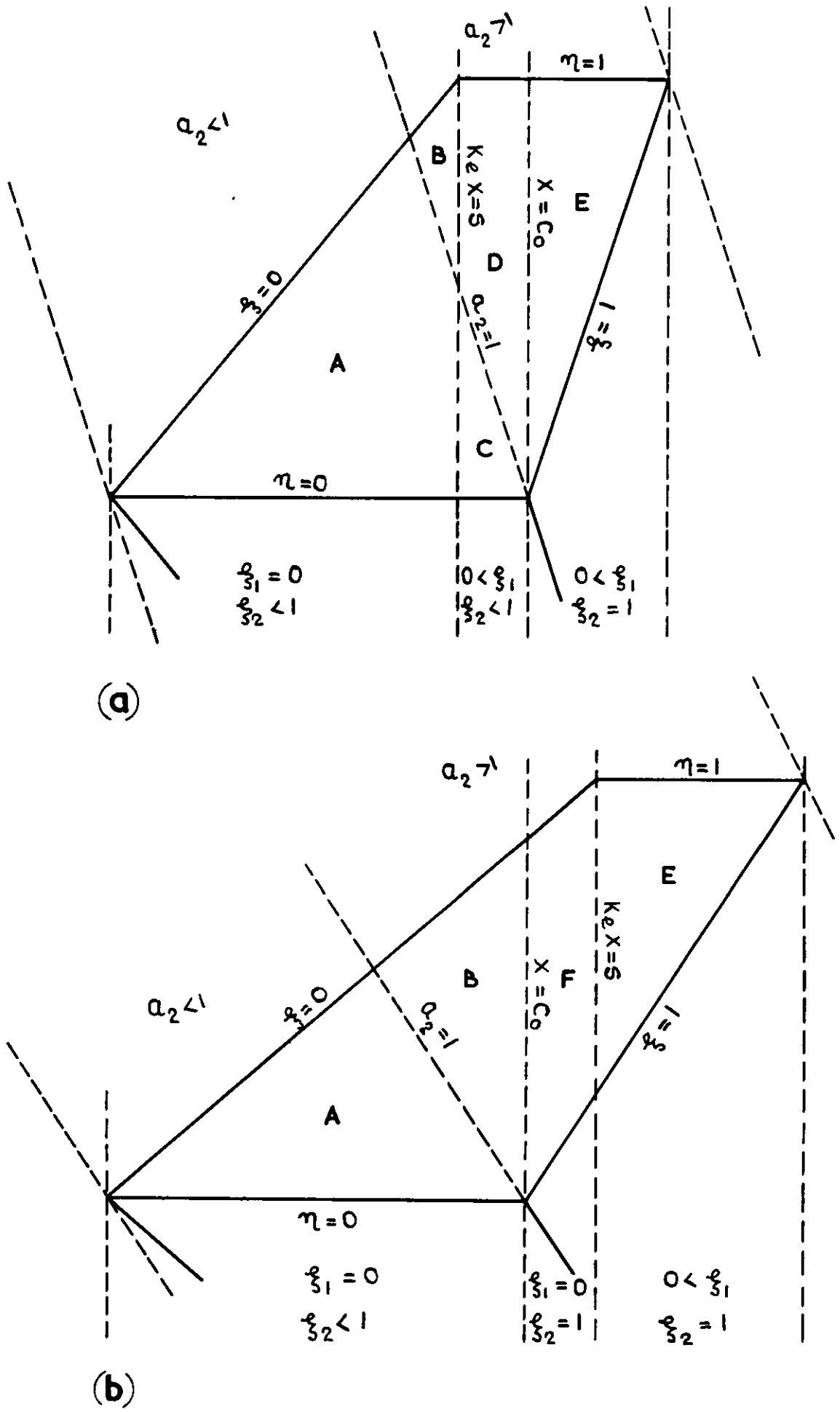

FIG. 3 (a & b) THE TWO TYPES OF SUB-DIVISION OF THE HALF-WING OCCURRING FOR SWEPT LEADING AND TRAILING EDGES.

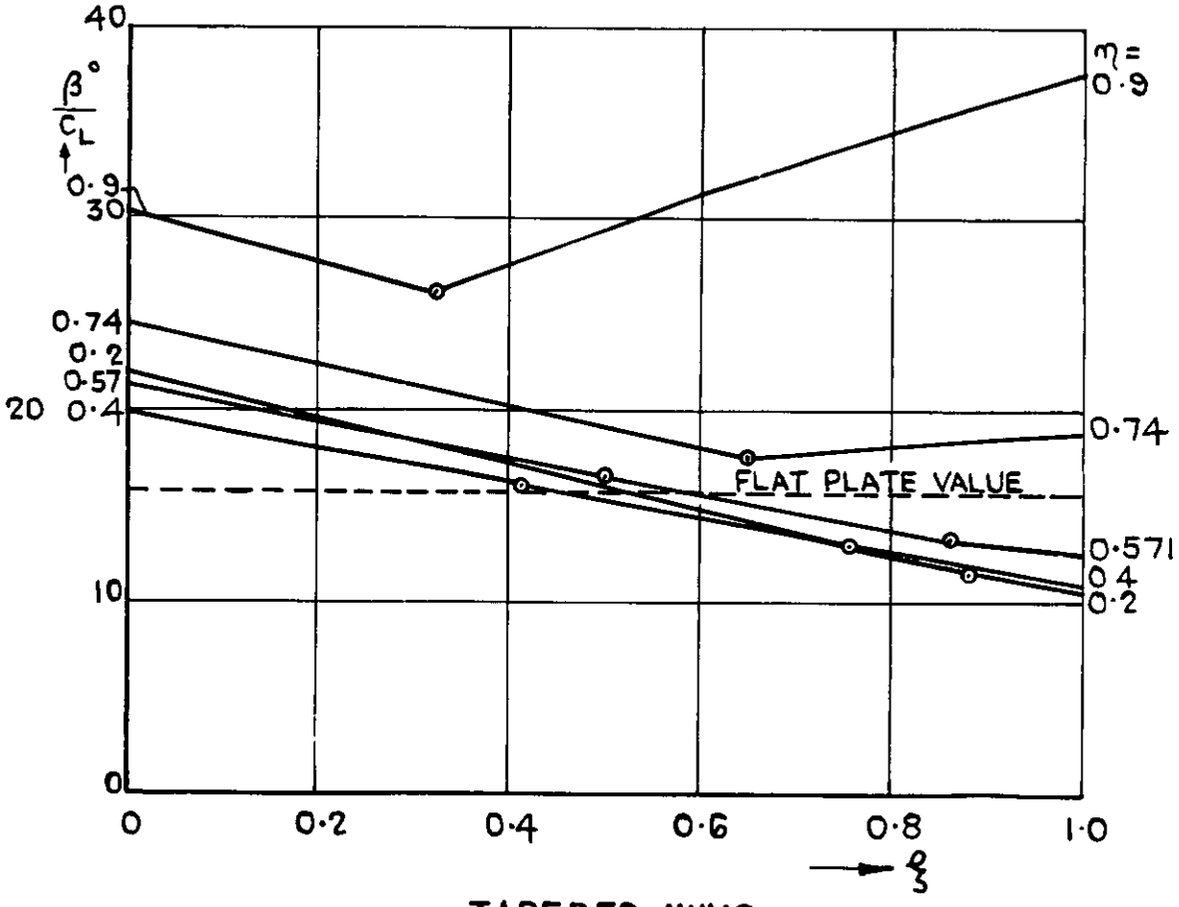

TAPERED WING.

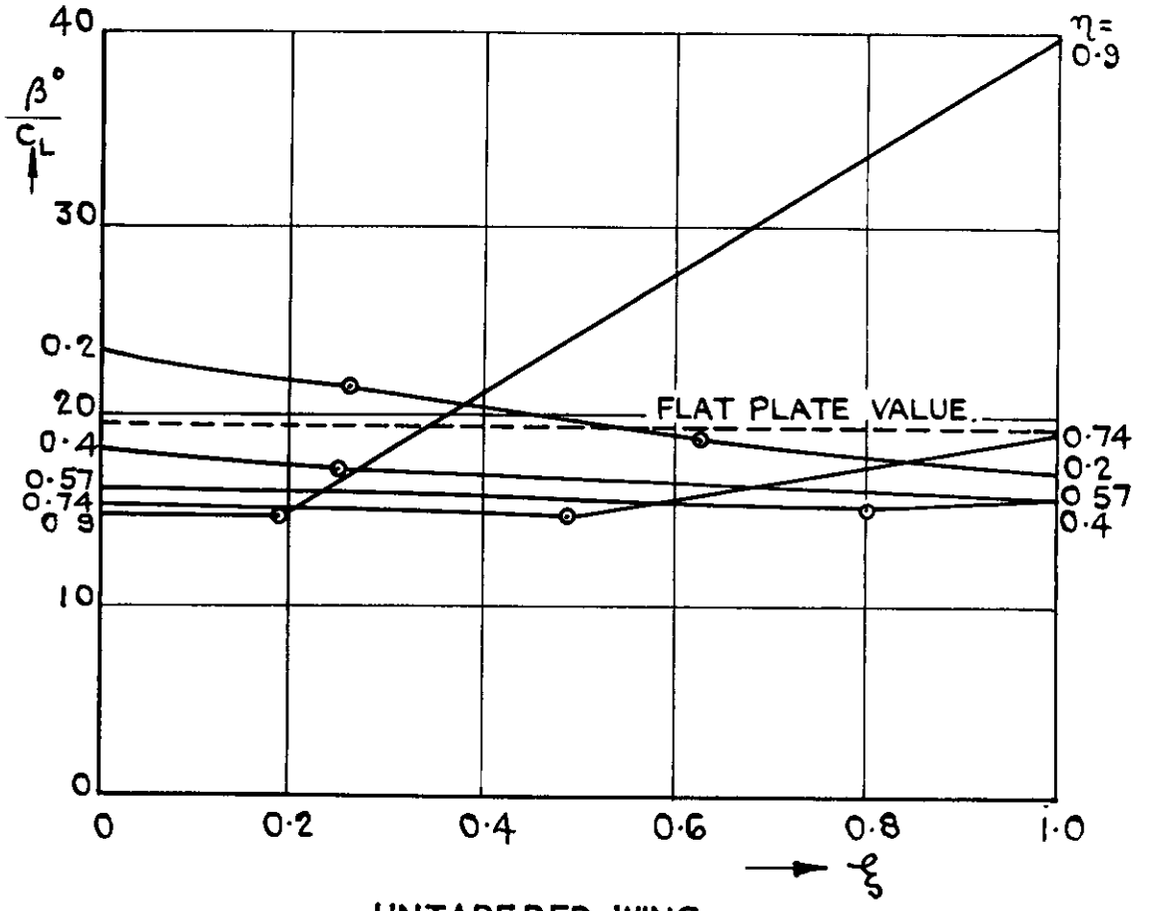

UNTAPERED WING.

FIG. 4. CHORDWISE VARIATION OF β/C_L FOR THREE STATIONS ON TWO WINGS WITH DISCONTINUITIES OF GRADIENT RINGED.

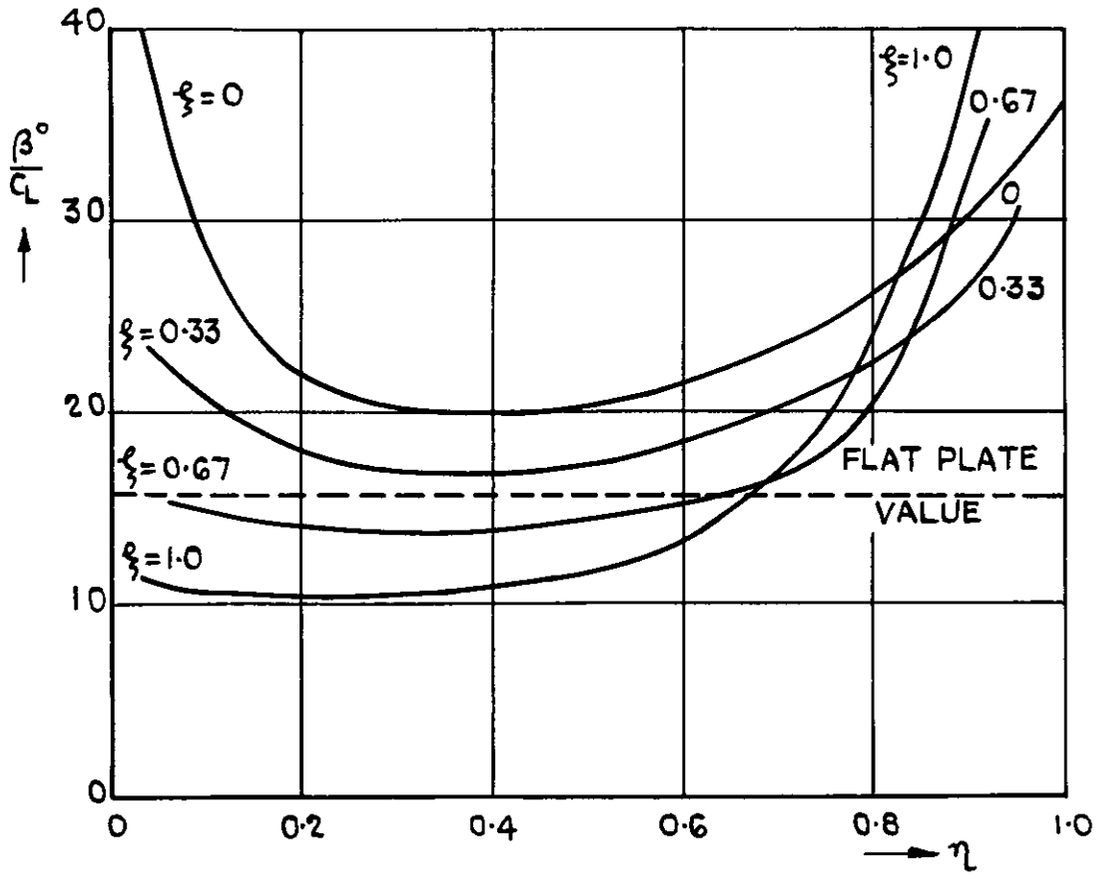

TAPERED WING

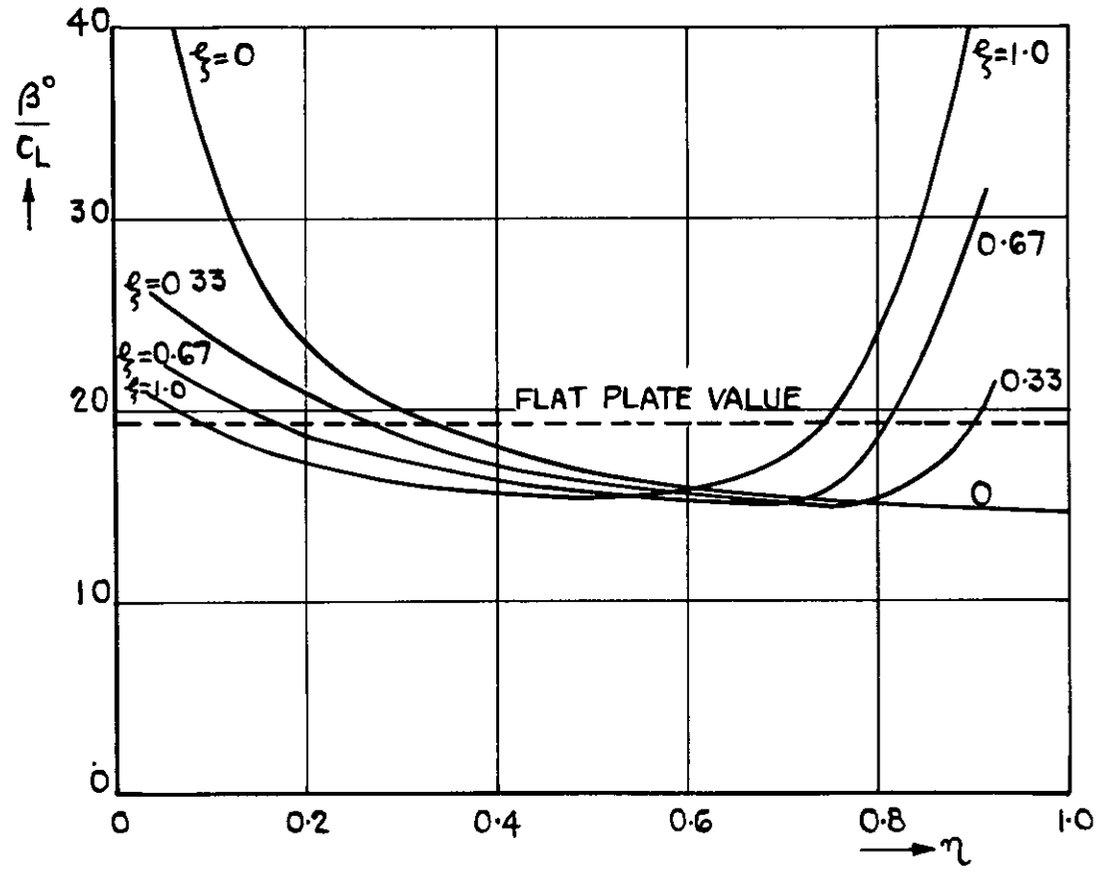

UNTAPERED WING.

FIG. 5. SWEEPWISE VARIATION OF β/C_L FOR ξ = CONSTANT.

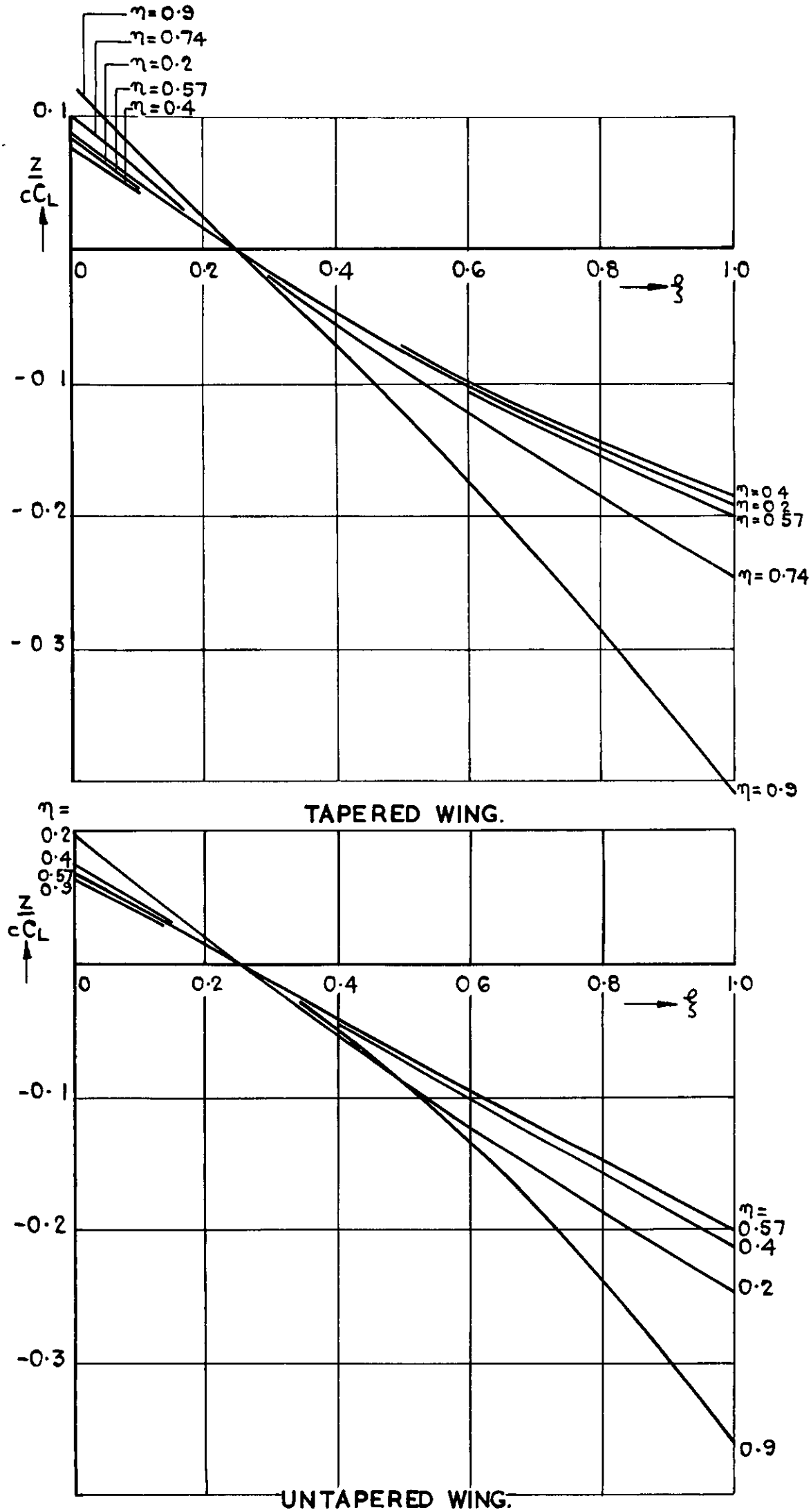

FIG. 6. CHORDWISE WING SECTIONS FOR THE WINGS AND STATIONS OF FIG. 4.

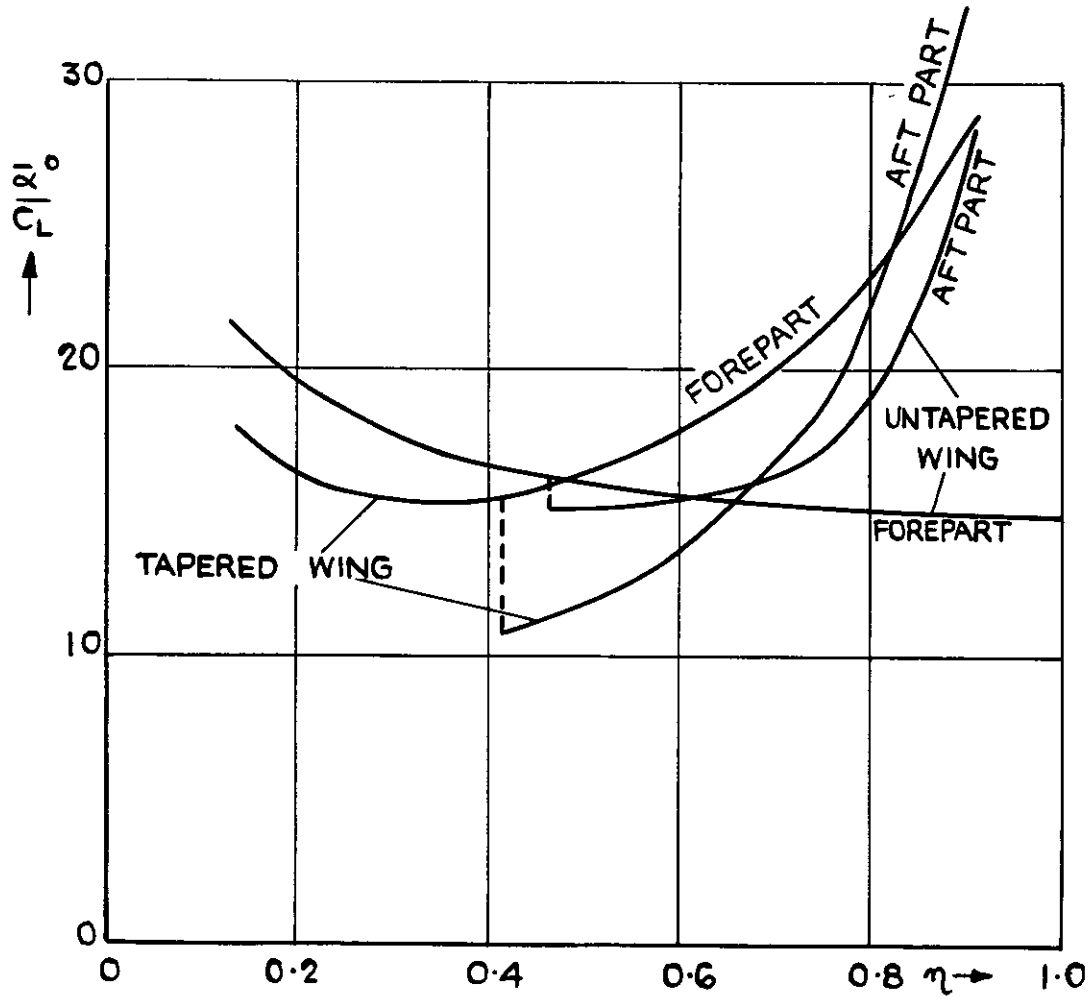

FIG. 7. SPANWISE LOCAL INCIDENCE DISTRIBUTION.

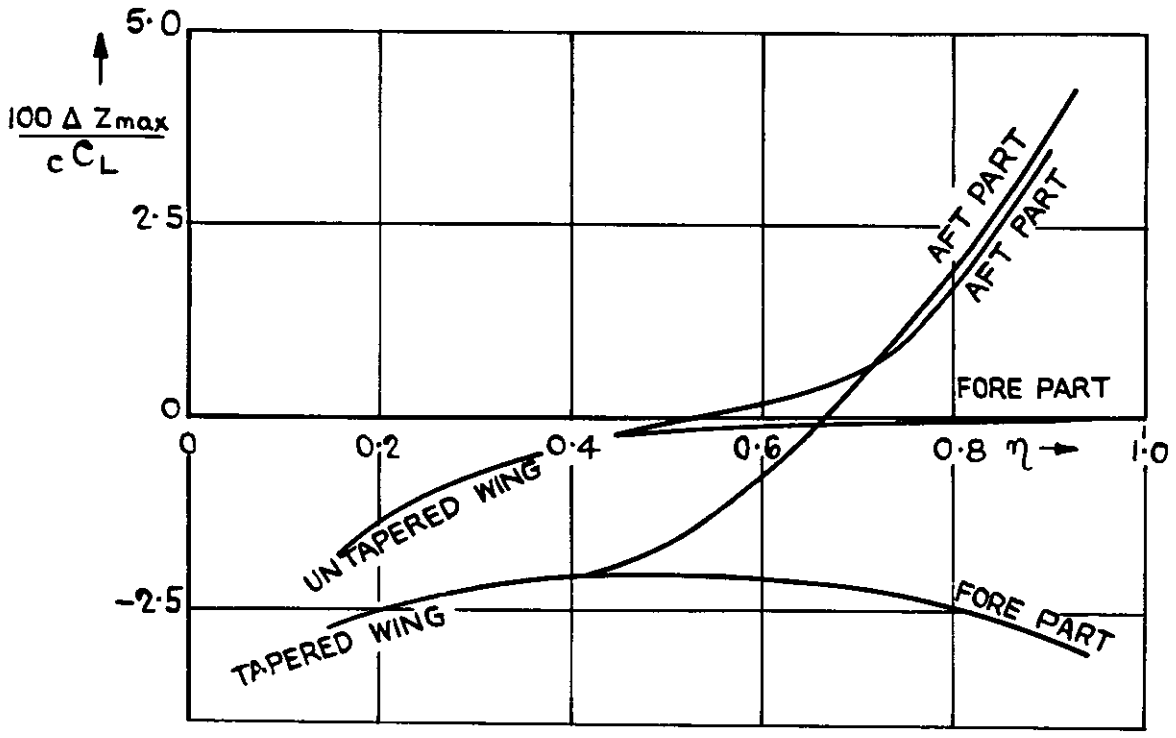

FIG. 8. SPANWISE CAMBER DISTRIBUTION.

C.P. No. 385
(18,755)
A.R.C. Technical Report

Published by
HER MAJESTY'S STATIONERY OFFICE

To be purchased from
York House, Kingsway, London W.C 2
423 Oxford Street, London W.1
13A Castle Street, Edinburgh 2
109 St. Mary Street, Cardiff
39 King Street, Manchester 2
Tower Lane, Bristol 1
2 Edmund Street, Birmingham 3
80 Chichester Street, Belfast
or through any bookseller

PRINTED IN GREAT BRITAIN

S.O. Code No. 23-9010-85

C.P. No. 385